Hydrophilic block copolymer-directed growth of lanthanum hydroxide nanoparticles

Frédéric Bouyer,[a] Nicolas Sanson,[a] Mathias Destarac[b] and Corine Gérardin*[a]

Received (in Montpellier, France) 18th November 2005, Accepted 21st December 2005
First published as an Advance Article on the web 25th January 2006
DOI: 10.1039/b516368d

Stable hairy lanthanum hydroxide nanoparticles were synthesized in water by performing hydrolysis and condensation reactions of lanthanum cations in the presence of double hydrophilic polyacrylic acid-b-polyacrylamide block copolymers (PAA-b-PAM). In the first step, the addition of asymmetric PAA-b-PAM copolymers ($M_{w,PAA} < M_{w,PAM}$) to lanthanum salt solutions, both at pH = 5.5, induces the formation of monodispersed micellar aggregates, which are predominantly isotropic. The core of the hybrid aggregates is constituted of a lanthanum polyacrylate complex whose formation is due to bidentate coordination bonding between La^{3+} and acrylate groups, as shown by ATR-FTIR experiments and pH measurements. The size of the micellar aggregates depends on the molecular weight of the copolymer but is independent of the copolymer to metal ratio in solution. In the second step, the hydrolysis of lanthanum ions is induced by addition of a strong base such as sodium hydroxide. Either flocculated suspensions or stable anisotropic or spherical nanoparticles of lanthanum hydrolysis products were obtained depending on the metal complexation ratio [acrylate]/[La]. The variation of that parameter also enables the control of the size of the core-corona nanoparticles obtained by lanthanum hydroxylation. The asymmetry degree of the copolymer was shown to influence both the size and the shape of the particles. Elongated particles with a high aspect ratio, up to 10, were obtained with very asymmetric copolymers ($M_{w,PAM}/M_{w,PAA} \geq 10$) while shorter rice grain-like particles were obtained with a less asymmetric copolymer. The asymmetry degree also influences the value of the critical metal complexation degree required to obtain stable colloidal suspensions of polymer-stabilized lanthanum hydroxide.

Introduction

Lanthanides are an attractive class of elements due to their electronic configuration and the related materials have interesting magnetic, optical, electrical, and nuclear properties that have applications in phosphors,[1–3] semiconductors[4–7] or biological detection[6,8] *etc*. Lanthanum, the lightest element in the lanthanide series, has been widely studied in its oxide, hydroxide, phosphate, or oxychloride forms for optical,[9,10] solid electrolyte,[11] catalytic,[12–16] and sorbent[17] properties. In order to improve the material properties, it is generally required to use particles in the nanometre scale with controlled shape and size as starting materials. Several methods have been described in the literature in order to obtain nanoparticles; they are well summarized in a recent paper.[18]

Organometallic approaches allow the synthesis of particles in the nanometric range; they may involve a reduction, an oxidation or a thermolysis step and, then, allow the preparation of metal or metal oxide nanoparticles.[19–23]

Template-based systems are also frequently used to control nucleation and growth of inorganic particles. Water-in-oil microemulsions were successfully used to prepare nanoparticles of controlled properties.[24–26] The synthesis is based on the formation of water droplets in an organic solvent; the nanoparticle size and shape are controlled by the chemical structure and concentration of surfactant. The use of reverse micelles with surfactants or amphiphilic block copolymers in an organic solvent is another effective route to prepare inorganic nanoparticles with various shapes (spheres, rods, platelets). The core of the preformed micelle serves as a metal salt host and is later submitted to metal ion reduction or hydrolysis depending on the targeted chemical phase.[26–29]

All the previously cited methods involve organic solvents as dispersing media. Due to environmental considerations, a great effort has to be made for the development of synthesis routes in aqueous solvent. For decades, the precipitation of inorganic particles in water from homogeneous solutions was shown to be an elegant way to obtain objects of desired size and shape. In the absence of metal chelating molecules the nanoparticle characteristics can be tuned by varying the nature of the counterion, the pH or the ionic strength.[30,31] Mineralization can also be controlled by using surface agents such as small chelating molecules or metal binding polyelectrolytes. Specific interactions between these molecules and preferential inorganic crystal faces allow the preparation of particles of

[a] *Laboratoire de Matériaux Catalytiques et Catalyse en Chimie Organique, UMR 5618 CNRS-ENSCM-UM1, FR 1878, Institut Gerhardt, 8 rue de l'Ecole Normale, 34296 Montpellier Cedex 5, France. E-mail: gerardin@enscm.fr; Fax: +33 4 67 16 34 70; Tel: +33 4 67 16 34 65*
[b] *Centre de Recherches Rhodia Aubervilliers, 93308 Aubervilliers, France*

different shapes.[32–34] The obtained particles are stabilized by electrostatic interactions, and the stability of these colloids is very sensitive to pH or ionic strength changes.

During the past few years, a new soft aqueous chemical route was proposed to synthesize inorganic particles using double hydrophilic block copolymers (DHBC). DHBC are composed of two water-soluble blocks of different chemical nature.[35,36] The case in which one block is ionizable and able to bind metal cations while the other one is neutral and serves as a stabilizer is particularly interesting. Such DHBCs were shown to be good candidates to control the crystal morphology of inorganic phases such as $CaCO_3$,[37,38] $BaSO_4$,[39] $CaPO_4$,[40] and CdS[41] but also to synthesize metallic nanoparticles such as Ag or Pt.[42,43] However, few publications refer to the preparation of metal hydroxide or oxide particles using DHBC.[44–46]

We previously showed that it was possible to synthesize lanthanum hydroxide and aluminium hydroxide particle suspensions by a two-step procedure using water-soluble block copolymers such as sodium polyacrylate-block-polyacrylamide (PAA-b-PAM) or sodium polyacrylate-block-polyhydroxyethylacrylate (PAA-b-PHEA).[44,46] In the case of lanthanum hydroxide, complexation of lanthanum ions by the polyacrylate block at a fixed pH induced the formation of micellar nanoaggregates. Then, the formation of mineralized lanthanum based nanoparticles was induced by addition of sodium hydroxide and hydroxylation of La^{3+} cations.

The present paper aims at studying the mechanisms involved in the synthesis of lanthanum hydroxide nanoparticles whose size and shape are influenced by the characteristics of the asymmetric PAA-b-PAM copolymers. First, the hydrolytic behaviour of lanthanum ions in the absence of polymer is presented. Indeed, the study of the pH-dependent speciation of lanthanum is a necessary step in order to establish the best conditions for La ion complexation by the copolymer. Then the properties of PAA-b-PAM copolymers in water solution are described. The formation of lanthanum based nanoaggregates by mixing copolymer and La^{3+} ions is studied using pH titration, IR spectroscopy, dynamic light scattering (DLS), and transmission electron microscopy (TEM). The transformation of the aggregates into mineralized hybrid particles by addition of a strong base is also investigated using DLS and TEM. Finally, the influence of pertinent parameters, such as the metal complexation degree and the copolymer molecular weight on the growth and the morphology of the hybrid colloids is explored. A series of copolymers with a high asymmetry degree ($M_{w,PAM}/M_{w,PAA} > 6$) is used in order to investigate the influence of the copolymer characteristics.

Experimental

Materials

$LaCl_3 \cdot 7H_2O$, $La(NO_3)_3 \cdot 6H_2O$, NaOH and polyacrylic acid (PAA 5100 g mol^{-1}) (Aldrich) were used as received. Ultrapure deionized water (MilliQ, Millipore, France) was used for all solution preparations. PAA-b-PAM copolymers were synthesized by free radical polymerization by Rhodia (Aubervilliers, France).[47] They were provided as aqueous solutions in acidic medium and were stored after lyophilization. Table 1 summarizes the characteristics of the different copolymers mentioned in the paper. In the following, the block copolymers are named by their molecular weights. In all copolymers, the ionizable block (PAA) is much shorter than the neutral block (PAM).

Table 1 Number of monomers in the different blocks of the PAA-b-PAM copolymers used in this work (block molecular weights are indicated as subscripts in the copolymer formulae)

Copolymers	n_{AA}	n_{AM}
PAA_{1000}-b-PAM_{10000}	14	145
PAA_{3000}-b-PAM_{10000}	42	145
PAA_{3000}-b-PAM_{30000}	42	435
PAA_{5000}-b-PAM_{30000}	70	435
PAA_{5000}-b-PAM_{60000}	70	869

Preparation of micellar aggregates and hybrid nanoparticles

The preparation of micellar aggregates and hybrid nanoparticles was conducted at room temperature. For the preparation of the micellar aggregates, an aqueous solution of lanthanum salt at 0.02 M in La^{3+} and 2.5 wt% solutions of PAA-b-PAM block copolymers were prepared as stock solutions at the same pH using NaOH. The required amount of polymer solution was added to 2 mL of lanthanum solution in order to adjust the complexation ratio R, which is the ratio between the number of acrylate groups [COO] and the number of lanthanum ions [La]. As a general rule, R ranged from 0 to 3. The mixture solution was stirred for 4 hours. The final volume was 4 mL, and the final concentration of lanthanum ions was 10^{-2} M.

Then, the solution of micelles was divided into two equal fractions: one was kept as it was. To the second fraction, 0.12 mL of NaOH 0.5 M was added slowly in order to induce hydrolysis of the metal cations and form the lanthanum based nanoparticles. Unless otherwise mentioned, the hydrolysis ratio, which is the total amount of hydroxyl ions added per lanthanum ion, was fixed at 3. The suspension was stirred for 1 night before further characterization.

Dynamic light scattering

DLS measurements were carried out by using a Zetasizer 3000HS instrument (Malvern, UK) with a 10 mW laser operating at 633 nm. All measurements were performed at 25 ± 0.2 °C. The samples were filtered through 0.22 μm filters (Millipore, France).

The diffusion coefficient of the particles, D, was calculated using the method of cumulants for polydisperse systems. The hydrodynamic diameter of the particles d_h was then obtained from the Stokes–Einstein equation:

$$d_h = \frac{k_B T}{3\pi\eta D} \quad (1)$$

where k_B is the Boltzmann constant, T is the absolute temperature, and η is the viscosity of the solvent

Electrophoretic mobility

The electrophoretic mobility of the particles was measured using a Zetasizer 3000HS instrument (Malvern, UK) with a 10 mW laser operating at 633 nm.

Small angle neutron scattering

SANS experiments were performed at the Leon Brillouin Laboratory (CEA/CNRS Saclay, France) using the PACE spectrometer. We used neutrons of wavelength $\lambda = 5$ Å and 10 Å at sample to detector distances of 3 and 10 meters. The instrument configurations allowed us to cover a range in the magnitude of the wave vector (q) from 0.004 to 0.5 $Å^{-1}$. Suspensions were introduced and analyzed in 2 mm thick quartz cells. Suspensions were prepared in D_2O to enhance the scattering length density differences between the solvent and the particles. The scattering data were corrected from background intensity. Scattering data are presented as a function of the magnitude of the scattering vector q.

Transmission electron microscopy

The suspensions were diluted 100 times and a drop was placed on a carbon–copper grid. After a few minutes of evaporation in air, the remaining solution was sucked with a filter paper to obtain a few particles or micelles on the grid. The sample was then characterized using a Jeol 1200 EXII microscope operated at 80 kV.

Attenuated total reflectance infrared spectroscopy

Infrared experiments were carried out using a Perkin-Elmer Spectrum 2000 ATR. Some drops of suspension were deposited on a diamond plate and the sample film was analyzed between 400 and 4000 cm^{-1}. 1000 scans and a resolution of 4 cm^{-1} were used for each experiment. Since the samples are mixtures of $La(NO_3)_3$ and copolymer, a reference spectrum of $NaNO_3$ solution at the same concentration in nitrate ions was subtracted in order to remove the bands characteristics of NO_3 groups that superimposed with the bands of the carboxylate groups of the copolymer.

Results and discussion

Hydrolysis of lanthanum salt

Due to its low charge to radius ratio, the lanthanum ion can easily be coordinated to a large number of water molecules. The hydration number is usually considered equal to 9 even if some discrepancies are found in the literature.[48,49] Hydrolysis of lanthanum ions leads to the replacement of coordinated water molecules by hydroxy-ligands and the formation of several hydrolysis species mentioned in Fig. 1.

Fig. 1 reports the fractions of these hydrolysis species as a function of pH considering the equilibrium constants given by Kragten and Decnopweever.[50] It is clearly seen that in acidic conditions (pH < 6.5) the hydrolysis of lanthanum ions is negligible. Above that critical pH value, several hydrolysis products coexist until pH 13 where $[La(OH)_4]^-$ is the only hydrolyzed species in solution. Around pH 10, $La(OH)_3$ is the dominant hydrolytic form with a very low solubility product ($K_s = 10^{-22.8}$).[50]

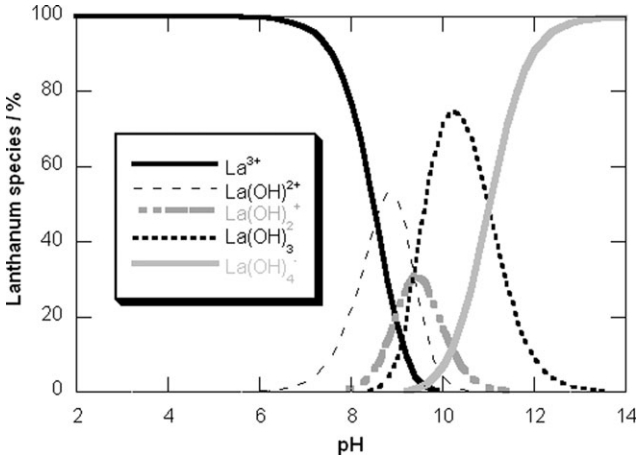

Fig. 1 Influence of pH on lanthanum speciation (equilibrium constant values from ref. 50).

The formation of polycations, $La_2(OH)^{5+}$ and $La_5(OH)_9^{6+}$, was proposed from pH measurements by Ciavatta and Biedermann[51] but their existence is the subject of controversy.[50,52,53] The different experimental conditions may explain the different points of view concerning the formation of polycations.

Fig. 2 reports the hydrolytic behavior of a 2×10^{-2} M $La(NO_3)_3 \cdot 6H_2O$ solution at room temperature by addition of 0.25 M NaOH. For a very low hydrolysis ratio ($h_1 = 0.08$) the pH reaches a plateau value (pH = 8.2) which is maintained up to a hydrolysis ratio of 2.5; the plateau is characteristic of lanthanum hydrolysis and condensation phenomena. In this regime, olation reactions may proceed and give rise to basic polynuclear species with a general formula $La_q(OH)_p^{(3q-p)+}$ as described by Biedermann and Ciavatta.[51] Stable colloids were obtained with a mean hydrodynamic size between 50 and 80 nm, and they are highly positively charged. We could not successfully characterize those colloids by TEM because they agglomerated during drying. Above OH/La = 2.9, macroscopic precipitation of lanthanum hydroxide occurs. Note that close to OH/La = 3, the pH equilibrates only after one night

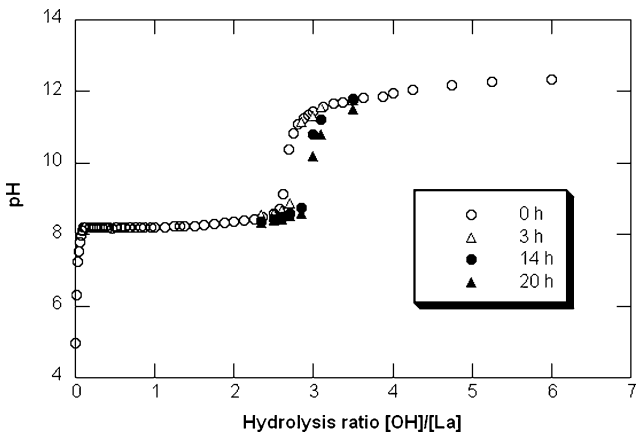

Fig. 2 Hydrolysis curve of a 2×10^{-2} M $La(NO_3)_3 \cdot 6H_2O$ solution by addition of 0.25 M NaOH.

(14 hours) as shown in Fig. 2. As a consequence, characterizations of the colloids were done after waiting for this period of time. That preliminary study allowed the set up of the conditions for the La complexation step by the copolymer and for the mineralization step.

Copolymers in solution

PAA-b-PAM block copolymers are hydrophilic polymers. All the copolymers used in this study are asymmetric, the length of the complexing block being shorter than the length of the solvating block (Table 1). The charge of the PAA block is pH dependent and the ionizable block is expected to coordinate multivalent metal cations. The neutral block, PAM, is not pH sensitive and its role consists in sterically stabilizing the colloids. In a previous work, we studied the behavior of such hydrophilic copolymers in water by DLS and SANS.[54] It was shown that at pH = 5.5 and in dilute conditions the asymmetric DHBC behave in water, in a first approximation, as neutral homopolymers in a good solvent considering excluded volume effects, and that they do not self-assemble.

Mixtures of lanthanum-based entities and copolymers: formation of micellar nanoaggregates

Various amounts of PAA_{5000}-b-PAM_{30000} copolymer solutions were added to a lanthanum chloride solution, both solutions being at pH 5.5. At this pH, the pre-hydrolysis ratio of lanthanum ions is negligible ($h_1 = [OH]/[La] = 5 \times 10^{-3}$) and the main species in solution is La^{3+} (see *Hydrolysis of lanthanum salt*). Besides, PAA blocks of the copolymer are half-ionized. Under these conditions, it is expected that the formation of micellar aggregates and the growth of particles are better controlled.

The mixture of the copolymer with the inorganic salt solutions leads to the formation of slightly opalescent suspensions which are stable for months whatever the complexation ratio. For comparison, mixing the same lanthanum salt solution with a solution of sodium polyacrylate ($M_{w,PAA}$ = 5100 g mol^{-1}) prepared at pH 5.5 results in the formation of a macroscopic precipitate. The phase separation is due to a chemical association between cations and acrylate groups that generates an insoluble complex by dehydrating the monomers and the cations.[55]

In the case of the mixture with the copolymer PAA_{5000}-b-PAM_{30000}, the opalescence results from the presence in water of objects denser than the copolymer itself. This agrees with our previous work using asymmetric PAA_{1000}-b-PAM_{10000} and PAA_{2800}-b-$PHEA_{11100}$ copolymers for which the structure of the colloidal objects was studied by SANS.[44] Mixing La^{3+} and asymmetric PAA-b-PAM or PAA-b-PHEA induces the formation of nanoaggregates due to the complexation of lanthanum ions by the polyacrylate blocks. It was previously shown that the nanoaggregates adopt a core-corona structure. The core is constituted of the lanthanum polyacrylate complex and is sterically protected by the neutral blocks of the copolymer. The formation of colloids with a similar structure was also proposed when noble metal ions, such as platinum or palladium ions, were added to an ionic-neutral DHBC solution.[42,43,56] The association of polyelectrolytes or surfactants

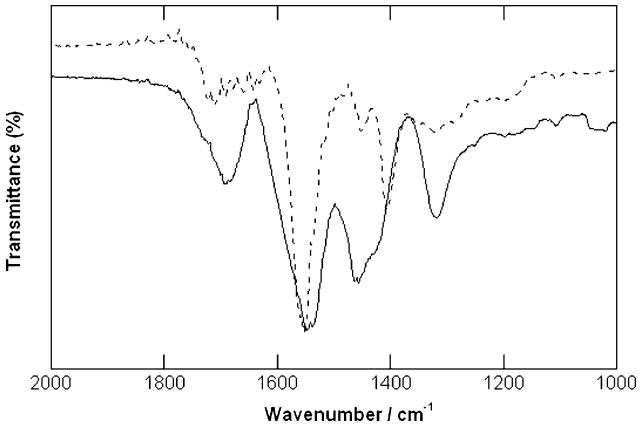

Fig. 3 ATR-FTIR spectra of PAA (5100 g mol^{-1}) homopolymer (dotted line) at pH 5.5 and a mixture La^{3+} + PAA (5100 g mol^{-1}) with a complexation ratio R = [COO]/[La] = 0.5 (solid line).

and oppositely charged DHBC also gives structures with a core-corona configuration where the core, composed of the two oppositely charged entities, is stabilized by the neutral blocks.[57–60]

We hereby further characterize the interactions between the PAA blocks and La^{3+} ions by ATR-FTIR measurements. Fig. 3 shows a comparison between the spectra of PAA_{5100} and the mixture $PAA_{5100} + La^{3+}$ (R = [COO]/[La] = 0.5) in water, all starting solutions having a pH fixed at 5.5. The PAA polyelectrolyte is partially ionized at pH 5.5. This is confirmed in Fig. 3 by the presence of vibrational bands located at 1406 and 1550 cm^{-1}, which are specific of the ionized groups of the polyacrylate ($\nu_{COO^-,antisym}$ and $\nu_{COO^-,sym}$, respectively) and the band at 1713 cm^{-1} due to the COOH groups ($\nu_{C=O}$).[61] After addition of lanthanum ions, the bands assigned to $\nu_{COO^-,antisym}$ and $\nu_{COO^-,sym}$ are shifted to 1419 and 1577 cm^{-1}, respectively, indicating the formation of a coordination bond between lanthanum ions and the acrylate groups. We also observed a decrease of $\Delta\nu_{COO^-} = \nu_{COO^-,antisym} - \nu_{COO^-,sym}$ upon addition of La^{3+}, which indicates that a bidentate coordination bond formed.[62] The two following reactions are possible:

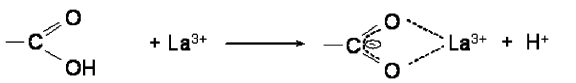

(2(a))

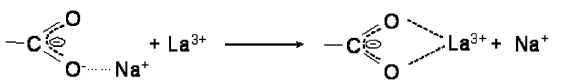

(2(b))

In case (2(a)) the coordination of La^{3+} to acrylic acid groups induces the release of protons in solution. This process is at the origin of the pH decrease which is systematically observed when PAA or PAA-based copolymers are mixed with La^{3+} solutions (pH of mixture = 3.2 at R = 1 for PAA_{5000}–PAM_{30000}).

Table 2 Hydrodynamic diameter (d_H) and polydispersity index (μ_2/Γ^2) and scattering intensity of micelles formed by complexation of La^{3+} by PAA_{5000}-b-PAM_{30000} copolymer ($[La^{3+}] = 10^{-2}$ mol L^{-1})

R = [COO]/[La]	0.2	0.5	0.8	1.0	2.0	3.0
d_H/nm	55.5	48.5	47	50.4	48.9	56
μ_2/Γ^2	0.11	0.12	0.05	0.06	0.07	0.10

ATR-FTIR experiments were also carried out on mixtures La^{3+}–PAA-b-PAM. However the spectra could hardly be exploited due to the absorption domain of NH_2 groups being close to that of acrylate and/or acrylic acid groups. Since the pH decrease is of the same order of magnitude when PAA-b-PAM or PAA homopolymer are added to lanthanum chloride solutions, we concluded that the solvating block does not influence the lanthanum–PAA interactions. So, it seems reasonable to expect the same bidentate bonding between La^{3+} and PAA blocks of the copolymer. That chelate bonding confers a great stability to the micellar aggregates. Indeed the size of the micellar aggregates, measured by DLS, remains unchanged when increasing the ionic strength up to 2.8 M. This is different from the case of polyion complex (PIC) micelles or block ionomer complexes (BIC) formed by association of oppositely charged organic entities for which supramolecular assemblies dissociate when the ionic strength exceeds 0.5 M.[63,64]

Table 2 reports the hydrodynamic diameters, d_H, and the polydispersity index, μ_2/Γ^2, of the aggregates obtained when mixing $LaCl_3$ and PAA_{5000}-b-PAM_{30000} solutions at pH 5.5 as a function of the complexation ratio, R. d_H remains fairly constant over the whole range of R and is equal to 51.1 ± 3.5 nm (see also Fig. 4). Furthermore, the micellar aggregates are fairly monodisperse since the polydispersity index does not exceed 0.12. Lanthanum based micelles were also synthesized with other PAA-b-PAM copolymers that have a similar asymmetry degree but different molecular weights (Table 3). Again, for a given DHBC, the size remains constant over the whole copolymer to metal ratio range. With PAA_{1000}-b-PAM_{10000}, we previously showed that micelles were predominantly spherical: the same morphology is also observed with PAA_{3000}-b-PAM_{10000} (Fig. 5). This result could be expected when considering the much larger volume of the stabilizing block relative to that of the insoluble part.[65] Fig. 5 reveals black dots, several of them being surrounded by grey circles. The black dots represent the micellar cores, which are the inorganic-rich parts of the aggregates and appear with a high contrast due to the concentration of La^{3+} ions. The grey

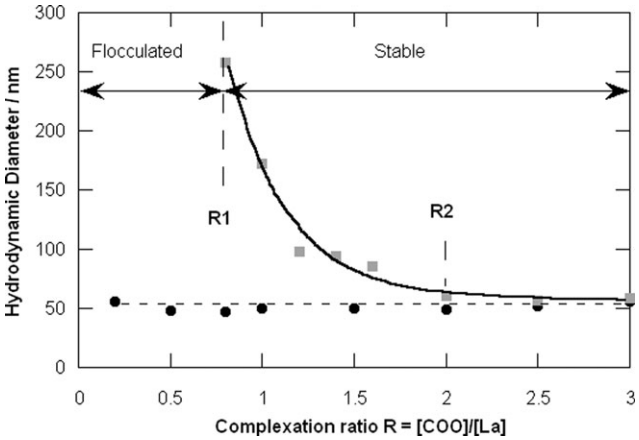

Fig. 4 Influence of the complexation ratio on the size of the precursor aggregates (●) and of the mineralized particles (■) in the system La^{3+}–PAA_{5000}-b-PAM_{30000}. The curves in the graph serve as eye guides.

diffuse circles around the darker dots represent the corona of neutral polymer blocks; it is well shown that the coronas prevent La^{3+}-rich nanodomains from coalescing and giving precipitation. The size of the black dots is about 5 nm, while the size of the whole aggregates (core + corona) is close to 15 nm. This value is smaller than the hydrodynamic diameter (25 nm) of the aggregates in water, which is expected since the corona may shrink upon drying on the TEM grid.

Several studies investigated the influence of the ions/DHBC ratio on the micellar size and various results were published. Li *et al.* noticed that the concentration of barium or calcium ions in a PEO-b-PMA solution did not change the hydrodynamic size of the colloids above a given degree of neutralization (DN) which is defined as $1/R$.[66] Furthermore, a critical aggregation concentration (*cac*) was identified, whose value (the same value for both cations) was shifted to lower DN as the copolymer concentration increased. In our study, no *cac* was observed, maybe due to the higher polymer concentration and the smaller complexation ratios that were used. Bronstein *et al.* observed that an increase in gold salt ($AuCl_3$) loading in PEO-b-PEI solutions scarcely influences the metal–polymer micelle size, while the incorporation of increasing amounts of H_2PtCl_6 in a solution of PEO-b-PEI induces an increase of the micellar size.[42] In the former case, micelle formation is a result of a ligand exchange of Cl or OH in the aqueous $[AuCl_3(OH)]^-$ anion by NH groups, while in the latter case, protonation of NH groups occurs first, accompanied by hydrogen bonding

Table 3 Hydrodynamic diameter (nm) of micellar aggregates formed by complexation of La^{3+} by various PAA-b-PAM copolymers ($[La^{3+}] = 10^{-2}$ mol L^{-1})

	Complexation ratio R = [COO]/[La]								
PAA-b-PAM	0.1	0.2	0.3	0.5	0.8	1	1.5	2	3
PAA_{1000}-b-PAM_{10000}	27.5	24.2	23.5	22	26.4	20	26.4	24.3	24.2
PAA_{3000}-b-PAM_{10000}	24.2	—	—	24.6	—	23.2	—	24.4	26.5
PAA_{3000}-b-PAM_{30000}	49.6	—	48.5	48.4	53.4	53.5	—	—	—
PAA_{5000}-b-PAM_{30000}	49.6	55.5	—	48.5	47	50.4	50.5	48.9	56
PAA_{5000}-b-PAM_{60000}	87.2	—	74.5	82.8	86.8	71.6	—	—	—

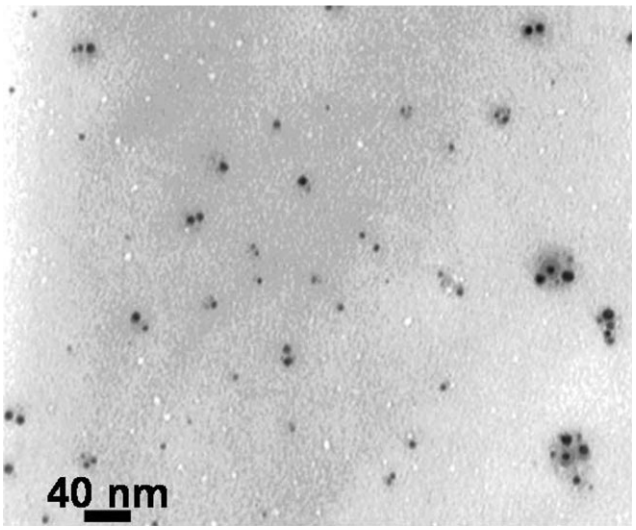

Fig. 5 TEM image of La^{3+} + PAA_{3000}-b-PAM_{10000} micellar aggregates (R = 1).

and electrostatic interaction between $PtCl_6^{2-}$ anions and NH_2^+ groups.

The electrophoretic mobility of the La^{3+}–PAA_{5000}-b-PAM_{30000} micellar aggregates was measured as a function of the complexation ratio, it is reported in Fig. 6. The values are very low but we can however notice that the electrophoretic mobility is slightly positive at low R values and regularly decreases when R increases from 0.1 to 0.8. Above R = 0.8, the electrophoretic mobility of the micellar aggregates becomes almost neutral. The low value of the electrophoretic mobility can be explained by the presence of the large neutral polymeric corona that slows down the migration of the micelles under the electric field. Also, the decrease of the mobility when R increases may be the result of the neutralization of the lanthanum charges by complexation with the acrylate groups of the copolymer.

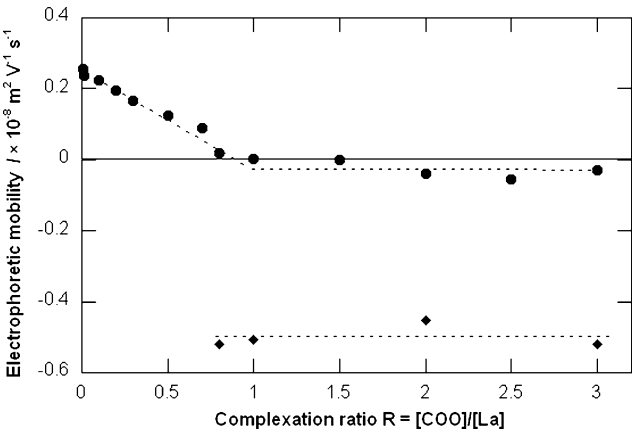

Fig. 6 Influence of the complexation ratio on the electrophoretic mobility of micelles (●) and mineralized particles (◆) for the system La^{3+}–PAA_{5000}-b-PAM_{30000}. The dashed lines in the graph serve as eye guides.

Hydrolysis of lanthanum ions in the La^{3+}–PAA_{5000}-b-PAM_{30000} system

In the mineralization step, preformed hybrid aggregates were used as precursors for the synthesis of lanthanum based particles. Considering that the metal pre-hydrolysis ratio was negligible ([OH]/[La] = 5×10^{-3}), three hydroxyl molecules per lanthanum ion were systematically added to the aggregate suspension in order to complete the lanthanum hydroxylation process. At constant lanthanum ion concentration, the copolymer content was varied so that the metal complexation ratio, R = [COO]/[La], varied between 0 and 3. The same processes were followed using different DHBC: PAA_{1000}-b-PAM_{10000}, PAA_{3000}-b-PAM_{30000}, PAA_{5000}-b-PAM_{30000}, and PAA_{5000}-b-PAM_{60000}. The different systems show similar trends: below a critical complexation ratio, $R1$, suspensions are flocculated; above $R1$, stable suspensions are obtained and no phase separation is observed, particle sizes of the stable colloids could then be measured. Fig. 4 shows the influence of the complexation ratio, R, on the particle size in the case of the La^{3+}–PAA_{5000}-b-PAM_{30000} system. As presented, there exists a value of R, $R2$, above which the size of the mineralized particles is similar to that of the precursor aggregates. Three domains can then be clearly distinguished:

(i) Below $R1$ = 0.8, flocculated suspensions are obtained. In this range of R, a large fraction of lanthanum ions is free in solution whereas the other part is involved in the formation of loose micelles which are slightly positively charged, as already mentioned (Fig. 6). When metal hydrolysis is completed by addition of NaOH, macroscopic precipitates form, due to the non-controlled precipitation of free La^{3+} ions. It was observed by TEM that very few elongated particles are embedded in the precipitate.

(ii) Between $R1$ and $R2$ = 2, stable colloidal suspensions are obtained. In that domain, the turbidity of the suspensions decreases when R increases. The hydrodynamic diameter of the colloids was measured by DLS and varies from 265 nm down to 55 nm when the complexation ratio R increases. Particle sizes are then higher than the precursor size (51.1 ± 3.5 nm). The morphology of the particles is strongly different

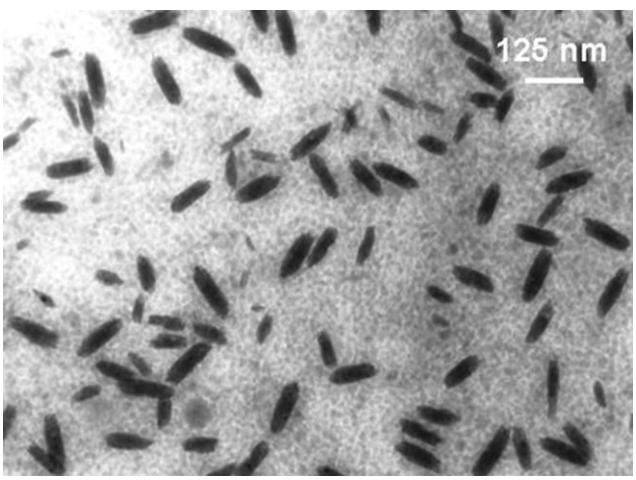

Fig. 7 TEM image of lanthanum-based particles in the presence of PAA_{5000}-b-PAM_{30000} (R = 1, h = [OH]/[La] = 3).

from that of the micelle precursor. Indeed rice grain-like particles (Fig. 7) were formed whereas the micellar precursors were isotropic. The formation of stable suspensions upon mineralization suggests that in the precursor micellar suspension, the fraction of free lanthanum ions in solution must be small. Otherwise a macroscopic precipitate would have formed since the solubility product of lanthanum hydroxide is very low. Upon addition of NaOH, hydrolysis of La^{3+} ions inside the micelle core proceeds and polycondensation reactions occur. The small fraction of free La^{3+} ions present in the precursor suspension certainly takes part in the hydrolysis and condensation phenomena. Free La^{3+} ions may come and feed the growing particles under mineralization. The micellar aggregates prepared at a complexation ratio below $R2 = 2$ are not stable upon hydrolysis and addition of OH^- leads to their coalescence: the particles grow until a critical copolymer amount is reached at the surface, which is sufficient to ensure particle stabilization. When R increases, precursor aggregates are richer in polymer and the fraction of free metal ions in solution is smaller. As a result, the amount of polymer per particle necessary to stop the coalescence process is reached more rapidly and the stable mineralized particles are then smaller. So, the growth of the particles is controlled by the DHBCs; the polymer amount governs the final particle size. Also, even if the polyacrylate block of the copolymer behaves as a poisoning agent of inorganic condensation reactions, the formation of elongated particles (Fig. 7) shows that particle growth is favoured in some specific directions. In that range of metal complexation ratios, micelles behave as open nanoreactors.

(iii) Above $R2$, the size of the particle remains constant, about 55 nm, and is the same as the size of the aggregate precursor. Furthermore, the particles are rather spherical as illustrated by Fig. 8. We can expect from the similitude in shape and size between the aggregates and the particles that inorganic polycondensation proceeds within the core of the micelle. The higher density of poisoning agents totally inhibits the outward particle growth and micelles behave as closed reservoirs of inorganic precursors. It was not possible to obtain a clear electronic diffraction pattern from those particles, which is not surprising considering the small size (9 nm) and the lack of crystallinity of the mineral particles. Nevertheless, it is expected that lanthanum hydroxide phase formed since the final pH of the suspension was 10. Indeed at this pH value, the predominant form of lanthanum species is $La(OH)_3$.

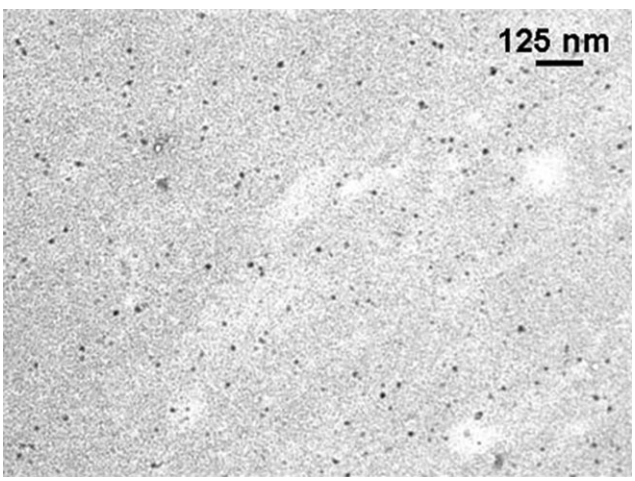

Fig. 8 TEM image of lanthanum-based mineralized nanoparticles prepared with PAA_{5000}-b-PAM_{30000} ($R = 3$, $h = 3$).

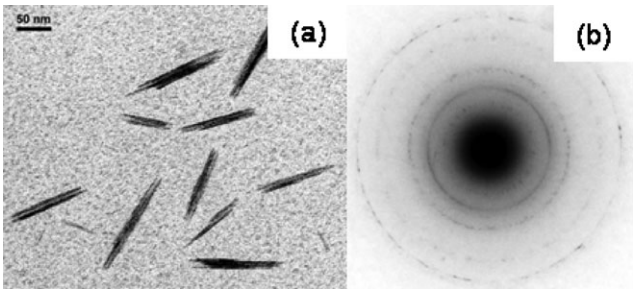

Fig. 9 TEM image of lanthanum-based nanoparticles in the presence of PAA_{1000}-b-PAM_{10000} ($R = 0.5$, $h = 3$) (a) and electron diffraction pattern of these colloids (b).

Characterization of the hairy mineralized nanoparticles obtained with different asymmetrical PAA-b-PAM copolymers

Between $R1$ and $R2$, anisotropic colloids were obtained upon lanthanum hydrolysis whatever the copolymer. In the case of the hydrolysis of the mixture $La(NO_3)_3$ + PAA_{1000}-b-PAM_{10000} ($R = 1$) the particles, shown in Fig. 9(a) have been characterized by electronic diffraction (ED). The diffraction pattern, reported in Fig. 9(b), shows that the lanthanum hydroxide $La(OH)_3$ phase was formed: the first, second, third and fifth diffraction rings, respectively correspond to the (100), (101), (201), and (211) planes. The formation of this phase is consistent with the value of the final pH of the suspension (pH = 10).

It is interesting to compare the shapes of the particles obtained using different copolymers (Fig. 7, 9(a), 10 and 11). Whereas very thin and sharp individual or packed particles are obtained with the PAA_{1000}-b-PAM_{10000}, PAA_{3000}-b-PAM_{30000} and PAA_{5000}-b-PAM_{60000} copolymers, particles synthesized with PAA_{5000}-b-PAM_{30000} exhibit rounded tips and have a lower aspect ratio: 3.5 compared to 8, 6.8 and 10.4 for the other asymmetrical copolymers, respectively. Experiments have been carried out using two different lanthanum salts, $LaCl_3$ and $La(NO_3)_3$, and the same morphologies were observed in the two cases. So, in the present synthesis route, the nature of the counterion seems not to influence the morphology of the lanthanum based particles. In this work, the

Table 4 Critical complexation ratio $R1$ for double hydrophilic block copolymers PAA-b-PAM with different asymmetries ($M_{w,PAA}/M_{w,PAM}$)

	$R1$	$M_{w,PAA}/M_{w,PAM}$
PAA_{5000}-b-PAM_{60000}	0.2	0.08
PAA_{1000}-b-PAM_{10000}	0.5	0.1
PAA_{3000}-b-PAM_{30000}	0.5	0.1
PAA_{5000}-b-PAM_{30000}	0.8	0.17

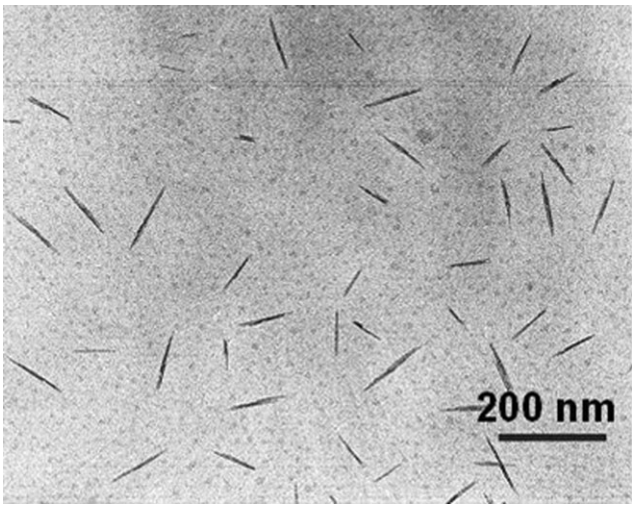

Fig. 10 TEM image of lanthanum-based nanoparticles in the presence of PAA_{5000}-b-PAM_{60000} ($R = 0.5$, $h = 3$).

asymmetry degree (molecular weight of the PAM block/molecular weight of the PAA block) of the copolymer is one of the main parameters that controls the particle shape: it seems that the higher the polymer asymmetry degree, the higher the particle aspect ratio is.

The asymmetry degree of the copolymer also influences the stabilization of the mineralized colloids. Indeed, the flocculation threshold, $R1$, is shifted to lower R values as the asymmetry of the copolymer increases (Table 4). Also, it is interesting to note that at a same complexation degree R, there are 1.67 times more AM neutral monomers with PAA_{1000}-b-PAM_{10000} than with PAA_{5000}-b-PAM_{30000} and this ratio is similar to the ratio between the respective $R1$ values, (0.8/0.5 = 1.6). That relation between $R1$ and the copolymer asymmetry degree shows the major role played by the neutral blocks in the colloidal stabilization phenomenon. This point will be developed in more details in a forthcoming paper.

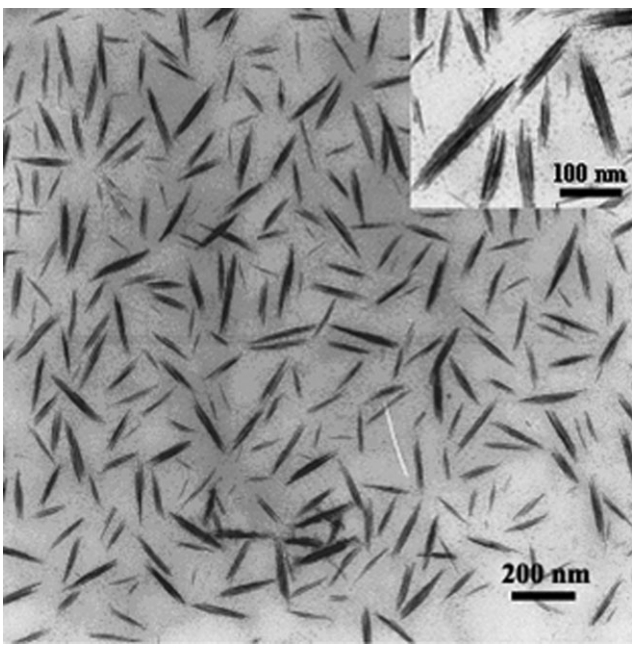

Fig. 11 TEM image of lanthanum-based nanoparticles in the presence of PAA_{3000}-b-PAM_{30000} ($R = 1$, $h = 3$).

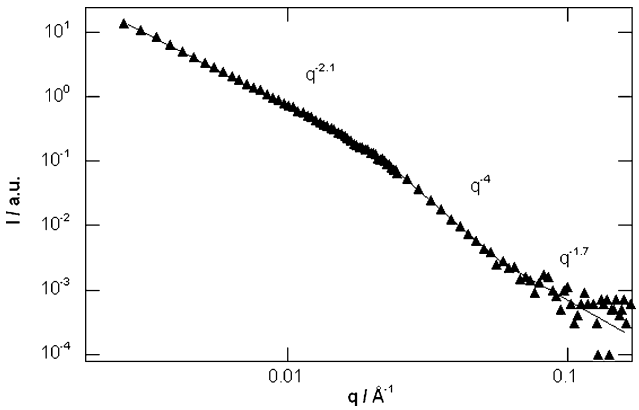

Fig. 12 Neutron scattering intensity *versus* scattering vector q obtained from lanthanum based nanoparticles with PAA_{1000}-b-PAM_{10000} copolymer ($R = 0.5$, $h = 3$).

The structure of the particles was characterized by SANS. Fig. 12 reports the SANS curve of lanthanum hydroxide particles synthesized in the presence of PAA_{1000}-b-PAM_{10000} copolymer. At high q values, the variation of the intensity as a $q^{-1.7}$ power law is characteristic of hairy particles: a polymer layer in a good solvent forms the particle corona. It is similar to that already observed with the micellar precursor.[44] It confirms that the copolymer remains attached to the mineral part of the particles upon lanthanum hydrolysis. The scattering curve also indicates that particles exhibit a flat surface ($I \propto q^{-2.1}$ at low q values), which seems to agree with the shape of the twinned particles shown in Fig. 9(a). At intermediate q values, a q^{-4} power law is observed; this power exponent is characteristic of the dense mineral core and of the sharp interface between $La(OH)_3$ and the polymer corona. The

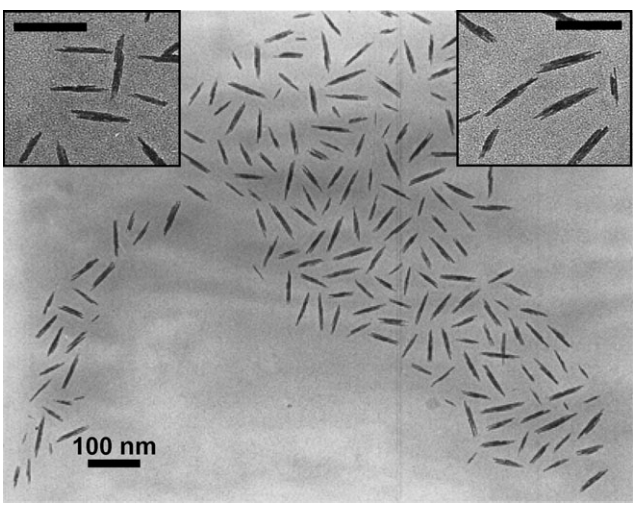

Fig. 13 TEM image of lanthanum-based nanoparticles in the presence of PAA_{1000}-b-PAM_{10000} ($R = 0.5$, $h = 3$).

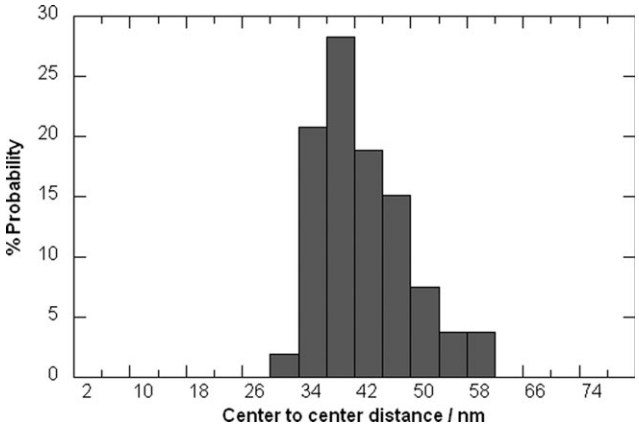

Fig. 14 Center to center distances of $La(OH)_3$ nanoparticles measured from Fig. 13.

presence of the polymer attached to the mineral particle was also evidenced by examining the variation of the particle hydrodynamic diameter when changing copolymers (d_H = 105 nm, 140 nm, and 334 nm, respectively for PAA_{1000}-b-PAM_{10000}, PAA_{3000}-b-PAM_{30000} and PAA_{5000}-b-PAM_{60000}, knowing that the mineral core lengths are, in all cases, comprised between 80 and 100 nm).

The stabilizing role of the hairy layer on the mineral particle could also be evidenced by Fig. 13 and 14. Fig. 13 displays a TEM image of $La(OH)_3$ nanoparticles obtained in the presence of PAA_{1000}-b-PAM_{10000} (R = 0.5, h = 3). The particles are well separated; they do not overlap and seem to be equidistant from each others. Using an image analysis software, all the distances between the centers of two parallel nanoparticles were measured and the results are reported in Fig. 14. The distribution of distances does not follow a Gaussian law; it is asymmetric. It exhibits a sharp increase at about 30 nm. Below this critical minimal distance, particles cannot get closer due to steric repulsions between the polymer chains. The critical distance of 30 nm corresponds to the minimal distance between hairy particles after a drying step. It is equal to the sum of twice the corona thickness plus the lanthanum particle width. After subtraction of the particle width (9 nm), it is found that the distance separating the particles equals 21 nm, which is a very reasonable value for twice the corona thickness knowing that the hydrodynamic diameter of the precursor micelle is 25 nm. It is also interesting to note that end-to-end aligned particles or those in normal directions with each other can get closer than particles in parallel directions. In such particular cases, distances smaller than 30 nm can be observed (see insets in Fig. 13). This would suggest an absence or a much lower density of polymer chains on the ends of the particles than on the sides, which favors the growth of particles along the longitudinal direction during the mineralization process. These observations allow us to get some new insight on the mechanisms of particle growth.

Conclusion

The synthesis of lanthanum hydroxide in the presence of various asymmetrical PAA-b-PAM copolymers has been studied. The procedure is divided into two steps. First, the addition of a copolymer solution to a lanthanum salt solution at pH 5.5 induces the formation of monodispersed and isotropic micellar hybrid aggregates. The aggregates adopt a core-corona structure: the core results from the complexation of lanthanum ions by the PAA blocks and is protected against coalescence and flocculation by the neutral PAM or PHEA blocks. ATR-FTIR experiments showed that bidentate coordination bonds exist between La^{3+} and the acrylate groups. The coordination reaction explains the strong decrease in pH after mixing lanthanum and copolymer solutions, both initially at pH 5.5. For a given copolymer, the size of the micellar aggregates does not depend on the complexation ratio, but increases with the molecular weight of the copolymer. In the second step, the addition of NaOH ([OH]/[La] = 3) to the suspensions of micellar aggregates induces the formation of either flocculated or stable suspensions of lanthanum hydroxide depending on the complexation degree. The value of the critical complexation degree, $R1$, that separates the two domains, is dependent on the asymmetry of the copolymer. The lower the asymmetry is, the lower $R1$ is. In the domain of colloid stability, the micellar precursors behave as opened ($R < R2$) or closed ($R > R2$) reservoirs in which hydrolysis and polycondensation of lanthanum ions occur. For $R1 < R < R2$, anisotropic nanoparticles are obtained and their size decreases as the complexation degree increases. Furthermore, the shape and the aspect ratio of the inorganic particles are controlled by the asymmetry degree of the copolymer. SANS characterization of the nanoparticles together with TEM results confirmed the presence of the copolymer at the surface. The high stability of the nanoparticles at high ionic strength is due to the strong coordination bonding. Above $R = R2$, the size and the shape of the nanoparticles are the same as those of the micellar precursor. In that case, the particle growth is prevented by a higher density of copolymer per micellar aggregate.

The present analysis of the formation mechanisms of the hairy nanoparticles should lead to a better control of the particle characteristics (size, shape, nanostructure). It has been shown that it is possible to prepare core-corona particles of metal ion hydrolysis products (metal oxide, hydroxide or basic salt) by controlled inorganic polycondensation reactions in suspension using new supramolecular assemblies as well-defined precursors.

Acknowledgements

F. Bouyer acknowledges financial support provided by Rhodia. The authors are grateful to Dr M. Granier (LCMOS, Montpellier) for his help in the characterization of the samples by ATR-FTIR. We also thank J. P. Selzner for the TEM images. Dr L. Auvray is also thanked for his help with neutron scattering experiments.

References

1 G. S. Yi, B. Q. Sun, F. Z. Yang, D. P. Chen, Y. X. Zhou and J. Cheng, *Chem. Mater.*, 2002, **14**, 2910–2914.
2 B. M. Tissue, *Chem. Mater.*, 1998, **10**, 2837–2845.

3 T. Jin, S. Inoue, S. Tsutsumi, K. Machida and G. Y. Adachi, *J. Non-Cryst. Solids*, 1998, **223**, 123–132.
4 A. R. Strzelecki, P. A. Timinski, B. A. Helsel and P. A. Bianconi, *J. Am. Chem. Soc.*, 1992, **114**, 3159–3160.
5 A. R. Strzelecki, C. L. Liker, B. A. Helsel, T. Utz, M. C. Lin and P. A. Bianconi, *Inorg. Chem.*, 1994, **33**, 5188–5194.
6 W. C. W. Chan, D. J. Maxwell, X. H. Gao, R. E. Bailey, M. Y. Han and S. M. Nie, *Curr. Opin. Biotechnol.*, 2002, **13**, 40–46.
7 J. N. Huiberts, R. Griessen, J. H. Rector, R. J. Wijnaarden, J. P. Dekker, D. G. deGroot and N. J. Koeman, *Nature*, 1996, **380**, 231–234.
8 C. Platas-Iglesias, L. Vander Elst, W. Z. Zhou, R. N. Muller, C. Geraldes, T. Maschmeyer and J. A. Peters, *Chem.–Eur. J.*, 2002, **8**, 5121–5131.
9 P. Schuetz and F. Caruso, *Chem. Mater.*, 2002, **14**, 4509–4516.
10 H. Meyssamy, K. Riwotzki, A. Kornowski, S. Naused and M. Haase, *Adv. Mater.*, 1999, **11**, 840–844.
11 N. Imanaka, K. Okamoto and G. Y. Adachi, *Angew. Chem., Int. Ed.*, 2002, **41**, 3890–3892.
12 A. Slagtern, Y. Schuurman, C. Leclercq and X. Verykios, *J. Catal.*, 1997, **172**, 118–126.
13 E. Ordonez-Regil, R. Drot, E. Simoni and J. J. Ehrhardt, *Langmuir*, 2002, **18**, 7977–7984.
14 S. J. Huang, A. B. Walters and M. A. Vannice, *J. Catal.*, 2000, **192**, 29–47.
15 C. H. Lin, K. D. Campbell, J. X. Wang and J. H. Lunsford, *J. Phys. Chem.*, 1986, **90**, 534–537.
16 P. Chanaud, A. Julbe, P. Vaija, M. Persin and L. Cot, *J. Mater. Sci.*, 1994, **29**, 4244–4251.
17 S. Tokunaga, S. A. Wasay and S. W. Park, *Water Sci. Technol.*, 1997, **35**, 71–78.
18 B. L. Cushing, V. L. Kolesnichenko and C. J. O'Connor, *Chem. Rev.*, 2004, **104**, 3893–3946.
19 (*a*) K. Pelzer, B. Laleu, F. Lefebvre, K. Philippot, B. Chaudret, J. P. Candy and J. M. Basset, *Chem. Mater.*, 2004, **16**, 4937–4941; (*b*) F. Dassenoy, K. Philippot, T. Ould-Ely, C. Amiens, P. Lecante, E. Snoeck, A. Mosset, M. J. Casanove and B. Chaudret, *New J. Chem.*, 1998, **22**, 703–711.
20 M. Verelst, T. O. Ely, C. Amiens, E. Snoeck, P. Lecante, A. Mosset, M. Respaud, J. M. Broto and B. Chaudret, *Chem. Mater.*, 1999, **11**, 2702–2708.
21 M. Monge, M. L. Kahn, A. Maisonnat and B. Chaudret, *Angew. Chem., Int. Ed.*, 2003, **42**, 5321.
22 M. C. Daniel and D. Astruc, *Chem. Rev.*, 2004, **104**, 293–346.
23 A. Labande, J. Ruiz and D. Astruc, *J. Am. Chem. Soc.*, 2002, **124**, 1782–1789.
24 I. Capek, *Adv. Colloid Interface Sci.*, 2004, **110**, 49–74.
25 D. H. Chen and S. H. Wu, *Chem. Mater.*, 2000, **12**, 1354–1360.
26 J. D. Hopwood and S. Mann, *Chem. Mater.*, 1997, **9**, 1819–1828.
27 L. Motte, C. Petit, L. Boulanger, P. Lixon and M. P. Pileni, *Langmuir*, 1992, **8**, 1049–1053.
28 M. P. Pileni, *Nat. Mater.*, 2003, **2**, 145–150.
29 E. E. Foos, R. M. Stroud, A. D. Berry, A. W. Snow and J. P. Armistead, *J. Am. Chem. Soc.*, 2000, **122**, 7114–7115.
30 E. Matijevic, *Chem. Mater.*, 1993, **5**, 412–426.
31 J. P. Jolivet, *Metal oxide chemistry and synthesis. From solution to solid state*, Wiley, Chichester, 2000.
32 T. Sugimoto, S. H. Chen and A. Muramatsu, *Colloids Surf., A*, 1998, **135**, 207–226.
33 F. H. Chen, H. S. Koo and T. Y. Tseng, *J. Am. Chem. Soc.*, 1992, **75**, 96–102.
34 S. H. Yu, H. Colfen, A. W. Xu and W. F. Dong, *Cryst. Growth Des.*, 2004, **4**, 33–37.
35 H. Cölfen, *Macromol. Rapid Commun.*, 2001, **22**, 219–252.
36 G. Riess, *Prog. Polym. Sci.*, 2003, **28**, 1107–1170.
37 J. Rudloff, M. Antonietti, H. Colfen, J. Pretula, K. Kaluzynski and S. Penczek, *Macromol. Chem. Phys.*, 2002, **203**, 627–635.
38 J. Rudloff and H. Colfen, *Langmuir*, 2004, **20**, 991–996.
39 M. Li, H. Colfen and S. Mann, *J. Mater. Chem.*, 2004, **14**, 2269–2276.
40 A. Peytcheva, H. Colfen, H. Schnablegger and M. Antonietti, *Colloid Polym. Sci.*, 2002, **280**, 218–227.
41 L. Qi, H. Coelfen and M. Antonietti, *Nano Lett.*, 2001, **1**, 61–65.
42 L. M. Bronstein, S. N. Sidorov, A. Y. Gourkova, P. M. Valetsky, J. Hartmann, M. Breulmann, H. Colfen and M. Antonietti, *Inorg. Chim. Acta*, 1998, **280**, 348–354.
43 S. N. Sidorov, L. M. Bronstein, P. M. Valetsky, J. Hartmann, H. Colfen, H. Schnablegger and M. Antonietti, *J. Colloid Interface Sci.*, 1999, **212**, 197–211.
44 F. Bouyer, C. Gérardin, F. Fajula, J. L. Putaux and T. Chopin, *Colloids Surf., A*, 2003, **217**, 179–184.
45 A. Taubert, D. Palms, Ö. Weiss, M.-T. Piccini and D. N. Batchelder, *Chem. Mater.*, 2002, **14**, 2594–2601.
46 C. Gérardin, N. Sanson, F. Bouyer, F. Fajula, J.-L. Putaux, M. Joanicot and T. Chopin, *Angew. Chem., Int. Ed.*, 2003, **42**, 3681–3685.
47 D. Taton, A. Z. Wilczewska and M. Destarac, *Macromol. Rapid Commun.*, 2001, **22**, 1497–1503.
48 W. Meier, P. Bopp, M. M. Probst, E. Spohr and J.-L. Lin, *J. Phys. Chem.*, 1990, **94**, 4672–4682.
49 P. A. Bergström and J. Lindgren, *Inorg. Chem.*, 1992, **31**, 1529–1533.
50 J. Kragten and L. G. Decnopweever, *Talanta*, 1987, **34**, 861–864.
51 G. Biedermann and L. Ciavatta, *Acta Chem. Scand. (1947–1973)*, 1961, **15**, 1347–1366.
52 T. Amaya, H. Kakihana and M. Maeda, *Bull. Chem. Soc. Jpn.*, 1973, **46**, 1720–1723.
53 P. K. Mohapatra and P. K. Khopkar, *Polyhedron*, 1989, **8**, 2071–2076.
54 N. Sanson, F. Bouyer, C. Gérardin and M. In, *Phys. Chem. Chem. Phys.*, 2004, **6**, 1463–1466.
55 I. Sabbagh and M. Delsanti, *Eur. Phys. J. E*, 2000, **1**, 75–86.
56 S. N. Sidorov, L. M. Bronstein, Y. A. Kabachii, P. M. Valetsky, P. L. Soo, D. Maysinger and A. Eisenberg, *Langmuir*, 2004, **20**, 3543–3550.
57 A. Harada and K. Kataoka, *Macromolecules*, 1998, **31**, 288–294.
58 T. K. Bronich, A. V. Kabanov, V. A. Kabanov, K. Yu and A. Eisenberg, *Macromolecules*, 1997, **30**, 3519–3525.
59 M. Moffitt, K. Khougaz and A. Eisenberg, *Acc. Chem. Res.*, 1996, **29**, 95–102.
60 J. F. Berret, G. Cristobal, P. Hervé, J. Oberdisse and I. Grillo, *Eur. Phys. J. E*, 2002, **9**, 301–311.
61 P. H. McCluskey, R. L. Snyder and R. A. Condrate, *J. Solid State Chem.*, 1989, **83**, 332–339.
62 K. Nakamoto, *Infrared and Raman Spectra of Inorganic and Coordination Compounds*, John Wiley & Sons, New York, 4th edn, 1986.
63 K. Kataoka, A. Harada and Y. Nagasaki, *Adv. Drug Delivery Rev.*, 2001, **47**, 113–131.
64 S. V. Solomatin, T. K. Bronich, T. W. Bargar, A. Eisenberg, V. A. Kabanov and A. V. Kabanov, *Langmuir*, 2003, **19**, 8069–8076.
65 J. N. Israelachvili, D. J. Mitchell and B. W. Ninham, *J. Chem. Soc., Faraday Trans. 2*, 1976, **72**, 1525–1568.
66 Y. Li, Y.-K. Gong and K. Nakashima, *Langmuir*, 2002, **18**, 6727–672.

